

Long-distance dynamical entanglement transfer via a chiral waveguide

Wai-Keong Mok,^{1,2,*} Davit Aghamalyan,² Jia-Bin You,¹
Wenzu Zhang,¹ Ching Eng Png,¹ and Leong-Chuan Kwek^{2,3,4}

¹*Department of Electronics and Photonics, Institute of High Performance Computing,
1 Fusionopolis Way, 16-16 Connexis, Singapore 138632, Singapore*

²*Centre for Quantum Technologies, National University of Singapore, 3 Science Drive 2, Singapore 117543*

³*MajuLab, CNRS-UNS-NUS-NTU International Joint Research Unit, UMI 3654, Singapore*

⁴*National Institute of Education and Institute of Advanced Studies,
Nanyang Technological University, 1 Nanyang Walk, Singapore 637616*

Quantum networks provide a prominent platform for realising quantum information processing and quantum communication, with entanglement a key resource in such applications. Here, we describe the transfer protocol for entangled states, where entanglement stored in the first node of quantum network can be transferred with high fidelity to the second node via a 1D chiral waveguide. In particular, we exploit the directional asymmetry in chirally-coupled single-mode ring resonators to transfer entangled states. For the fully chiral waveguide, the Bell state $|\Psi^+\rangle$ can be transferred with fidelity as high as 0.958. Using the same protocol, multipartite W states can be transferred with high fidelity. Our proposal can be utilised for long-distance distribution of multipartite entangled states between the quantum nodes in a quantum network.

Introduction.—Quantum networks [1, 2] provide a prominent platform for realising quantum information processing and quantum communication, with entanglement a key resource in such applications. Quantum networks consist of nodes, which are usually formed with atoms. Nodes are then linked together through the quantum channel via photons (referred in this picture as (“flying qubits”). In this context, the main task and at the same time an outstanding challenge is the high fidelity transfer of quantum states on long distances despite having noise and dissipation present in the quantum channel [3].

It is well known that if Bob shares entangled qubit pairs both with Alice and Carol, then by using classical communication channel, crucial protocols like teleportation [4], entanglement swapping [5, 6] and quantum cryptography [7, 8] can be achieved with high success rate. These breakthrough achievements demonstrate that entanglement is a vital ingredient for realizing quantum information and quantum communication tasks [3]. In this Letter we target a rather different question: if Bob, who is located in the first node of quantum network, has a known entangled state, how can he transfer (without using a classical communication channel) it to the Alice, who is located in the second node, with a high fidelity?

One such solution comes from using chiral waveguides. In quantum optics, chirality arises, for instance, in atom-waveguide coupled systems when the symmetry of photon emission in the left and right directions is broken [9]. This effect appears as a result of spin-orbit coupling, and has been experimentally demonstrated in plasmonic waveguides [10]. Chiral systems have been shown to be fruitful for realizing quantum networks [11–13] with the added feature that multipartite entangled states can be generated with almost all-to-all connectivity in the steady state. In Ref. [14] it was argued that maximum achiev-

able concurrence between two atoms is 1.5 times higher as compared to the non-chiral system with additional benefit that the generated entanglement is insensitive to the distance between the atoms.

Quite remarkably, these chiral systems in the case of perfect chirality realize the paradigm of cascaded systems, where two systems are coupled unidirectionally without information backflow. As was independently demonstrated by Gardiner and Carmichael [15–17], cascaded systems, even when they are separated by long distances, can be described under the Born-Markov approximation with retardation effects accounted for by a simple redefinition of the time and phase of the second node. Non-Markovian effects (due to the finite time delay between nodes) were shown to be detrimental for generating entangled states in atom-waveguide systems [18, 19]. Here, we exploit cascaded systems in the Born-Markov regime to achieve high-fidelity entanglement transfer.

To implement functional quantum networks, photonic quantum devices [20] are key components and play an important role in storing the quantum states of light. For example, micro-chip based systems such as micro-toroidal and microdisk cavities hold a promise to realize scalable quantum networks [21]. Moreover, by coupling tapered fibre with ring resonator, the coupling efficiency of light in and out of the microtoroidal resonator can be experimentally achieved up to 0.997 [22]. In Ref. [23] it was demonstrated that by introducing ring cavities in the atom-waveguide system it is possible to implement a quantum state transfer protocol which is immune to the thermal noise if the waveguide is perfectly chiral.

Several theoretical proposals [12, 23–31] as well actual experimental realizations [32–34] for the quantum state transfer of a single qubit in quantum optical networks have been put forward. For instance, in the seminal proposal by Cirac *et al.* [24], the qubit state is written in

a three-level atom and by applying control pulses, the state can then be transferred to the second node using a time-symmetric photonic wave packet, which mimics the reverse process of the wavepacket emission. In all aforementioned proposals, there are few demanding requirements that are hard to be met experimentally: external control pulses which have non-trivial temporal shapes, time-dependent cavity-atom and fiber-atom interaction strengths. Moreover, to the best of our knowledge, there are no existing protocols for long-distance entanglement transfer in the optical frequency domain.

On the other hand, spin chains can alleviate the issue of tricky control of system parameters and realize quantum systems with minimal control (coupling constants are fixed in time), and entanglement transfer has been demonstrated in several theoretical manuscripts [35–41] in the Heisenberg-type spin chains. However, these systems can only realize short-distance state transfer, as experimentally one is limited by the number of spins, and it is also widely believed that increasing the length of a spin chain will worsen transfer fidelities due to dispersion effects.

Motivated by Refs. [14, 23], we harness unidirectional coupling introduced by the chiral waveguide, which serves as a platform for realising cascaded system dynamics governed by the Markovian dynamics, which hold even for nodes that are separated by large distances. By coupling ring cavities with chiral 1D waveguide, we demonstrate entanglement transfer, with the entangled state stored in the atomic ensembles which are coupled to the ring cavities. It is important to highlight that ring cavities provide greater control over the system compared to the bare atom-fiber coupled case, where the transfer fidelity is significantly lowered due to long-range interactions between the atoms. Consequently, one node of our quantum network consists of an atomic ensemble which is coupled to the ring cavity. Communication channel is realized with a chiral waveguide. We demonstrate the transfer maximally entangled Bell states and W -states with up to 5 qubits. W -states are extremely useful for quantum information and communication applications as they are more robust states for encoding single qubit states. Moreover, W -states have the unique property (contrary to say, GHZ states) that even if one particle is lost, the rest of $N - 1$ qubits will remain in the entangled state.

Compared to other schemes, our proposal has various advantages. Firstly, the scheme works in the weak coupling regime with no external driving field required. Also, the optimal transfer of entanglement occurs dynamically, which can potentially lead to faster transfers compared to steady state schemes [11]. On top of that, by using chirality, the entanglement transfer is not sensitive to the distance between the atoms. Moreover, by using a perfectly chiral waveguide, our proposal is valid for long-distance entanglement transfer since in cascaded systems the time delay between nodes is manifested as a simple retarda-

tion effect. We comment that although non-Markovian effects should in general be taken into account if one consider long distances with imperfect chirality, this is not required here as long as the entanglement is transferred much faster than the timescale for information backflow to occur. Our results indicate that such conditions can be easily achieved for long-distance waveguides.

Chiral waveguide QED system.—The system in consideration consists of two nodes coupled to a 1D waveguide. Each node comprises of N qubits coupled to a single cavity mode. The Hamiltonian for this system is given by $H = H_S + H_B + H_{SB}$, with (setting $\hbar = 1$)

$$\begin{aligned}
H_S &= \sum_{j=1}^2 \sum_{l=1}^N [\omega_l^{(j)} \sigma_l^{(j)\dagger} \sigma_l^{(j)} + \omega_{cj} a_j^\dagger a_j \\
&\quad + g_l^{(j)} (a_j^\dagger \sigma_l^{(j)} + \text{H.c.})] \\
H_B &= \sum_{\lambda=L,R} \int d\omega \omega b_\lambda^\dagger(\omega) b_\lambda(\omega) \\
&\quad + \sum_{j=1}^2 \sum_{l=1}^N \int d\omega \omega b_l^{(j)\dagger}(\omega) b_l^{(j)}(\omega) \\
H_{SB} &= i \sum_{j=1}^2 \sum_{\lambda=L,R} \int d\omega \sqrt{\frac{\gamma_\lambda}{2\pi}} \left(b_\lambda^\dagger(\omega) e^{-ikx_j} a_j - \text{H.c.} \right) \\
&\quad + i \sum_{j=1}^2 \sum_{l=1}^N \int d\omega \sqrt{\frac{\Gamma_{jl}}{2\pi}} \left(b_l^{(j)\dagger}(\omega) \sigma_l^{(j)} - \text{H.c.} \right)
\end{aligned} \tag{1}$$

where the transition frequencies of the qubits and resonant frequency of the cavity are $\omega_l^{(j)}$ and ω_{cj} respectively. The atom-cavity coupling strength is given by $g_l^{(j)}$.

The bosonic operators for the cavity mode are a_j^\dagger and a_j , satisfying the canonical commutation relation $[a_j, a_{j'}^\dagger] = \delta_{jj'}$. The waveguide is treated as a common reservoir, with bosonic operators $b_\lambda^\dagger(\omega)$ and $b_\lambda(\omega)$ satisfying the commutation relation $[b_\lambda(\omega), b_{\lambda'}^\dagger(\omega')] = \delta_{\lambda\lambda'} \delta(\omega - \omega')$. The interaction strength between the cavities and the waveguide (at position x_j) is characterised by the decay rate γ_λ . Here we assume that the cavities do not decay into non-waveguide modes, which can be realised in plasmonic waveguides with high β -factors [42–44].

The spontaneous decay of the qubits is described by an interaction with independent baths at a decay rate Γ_{jl} , where the first index denotes the cavity and the second index denotes the qubit. The bath operators $b_l^{(j)\dagger}(\omega)$ and $b_l^{(j)}(\omega)$ satisfy the commutation relation $[b_l^{(j)}(\omega), b_{l'}^{(j')\dagger}(\omega')] = \delta_{jj'} \delta_{ll'} \delta(\omega - \omega')$.

By tracing out the waveguide mode, and applying the Born-Markov approximation, the Lindblad master equation for the system can be found as [11] (details are in

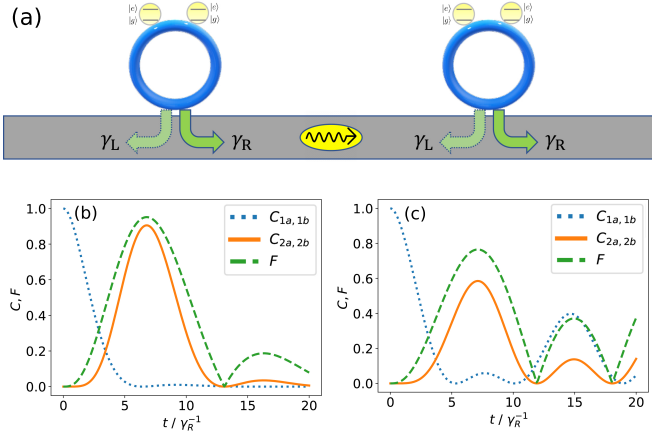


FIG. 1. (a) The proposed setup for entanglement transfer. Each node comprises N qubits ($N = 2$ in the figure) coupled to a single cavity mode. Chirality is enforced by setting $\gamma_L \neq \gamma_R$. Concurrence for the transfer of Bell state $|\Psi^+\rangle$. (b) Chiral coupling with $\gamma_L = 0$ (c) Non-chiral coupling with $\gamma_L = \gamma_R$ and $kD = \pi$. Cavity-atom coupling is set at the optimal value $g_1 = g_2 = 0.3\gamma_R$.

Appendix A

$$\begin{aligned} \dot{\rho} = & -i[H_{\text{eff}}, \rho] + \gamma_L \mathcal{D}[e^{ikx_1} a_1 + e^{ikx_2} a_2] \rho \\ & + \gamma_R \mathcal{D}[e^{-ikx_1} a_1 + e^{-ikx_2} a_2] \rho + \sum_{j,l} \kappa_{jl} \mathcal{D}[\sigma_l^{(j)}] \rho \end{aligned} \quad (2)$$

with the effective Hamiltonian

$$\begin{aligned} H = & \sum_{j,l} [\omega_l^{(j)} \sigma_l^{(j)\dagger} \sigma_l^{(j)} + \omega_{cj} a_j^\dagger a_j + g_l^{(j)} (a_j^\dagger \sigma_l^{(j)} + \text{H.c.})] \\ & - i \frac{\gamma_L}{2} (e^{ikD} a_1^\dagger a_2 - \text{H.c.}) - i \frac{\gamma_R}{2} (e^{ikD} a_2^\dagger a_1 - \text{H.c.}) \end{aligned} \quad (3)$$

where $D = |x_2 - x_1|$ is the distance between the nodes. In the following, we will study the transfer of entangled qubit states between the nodes mediated by the waveguide. The case of $N = 2$ is first presented to illustrate Bell state transfer.

Transfer of Bell states with chiral couplings.—Here, we exploit the directional asymmetry by using a chiral light-matter interface, with $\gamma_L = 0, \gamma_R \neq 0$ [23]. Using chiral couplings, the setup is essentially a cascaded quantum system [15] where the first node is coupled to the second node unidirectionally without backflow of information. In this case, the setup we consider can be used to study long-distance entanglement transfer despite the Born-Markov approximation used, since retardation effects in a cascaded quantum system is accounted for by a simple redefinition of the time of the second node [17].

For simplicity, we assume that the qubits do not decay ($\kappa_{jk} = 0$), and the nodes are identical, i.e. $\omega_k^{(j)} = \omega_0$,

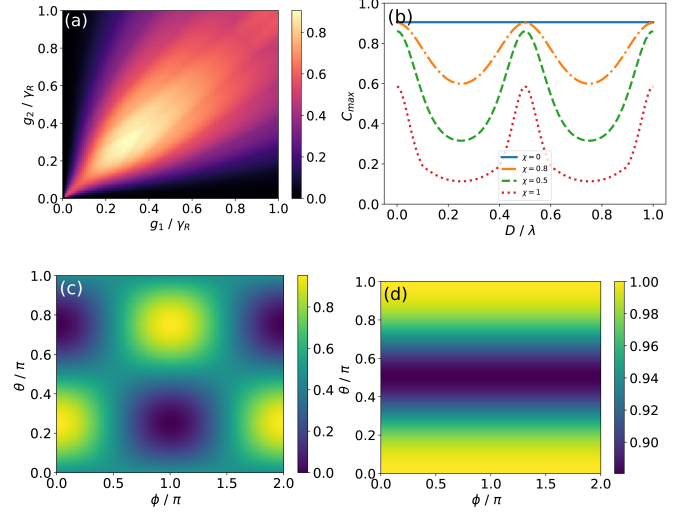


FIG. 2. (a) Maximum concurrence of $2a, 2b$ against g_1, g_2 shows optimal point $g_1 = g_2 = 0.3\gamma_R$. (b) Maximum concurrence of $2a, 2b$ against inter-nodal distance D . (c) Maximum transferred fidelity of $2a, 2b$ against various initial states $|\psi_1\rangle$. Maximum transferred fidelity of $2a, 2b$ against various initial states $|\psi_2\rangle$. Other parameters are: $g_1 = g_2 = 0.3\gamma_R$

$\omega_{cj} = \omega_c, g_k^{(j)} = g_j$, for all $j, k \in \{1, 2\}$. The qubits in the first node are denoted by $1a, 1b$ while the qubits in the second node are denoted by $2a, 2b$. We first prepare the qubits $1a, 1b$ in the Bell state $|\Psi^+\rangle = \frac{1}{\sqrt{2}}(|eg\rangle + |ge\rangle)$, and consider resonant conditions $\omega_c = \omega_0$ with cavity coupling strength $g_1 = g_2 = 0.3\gamma_R$.

As shown in Fig. 1(b), the concurrence of $1a, 1b$ decreases to near zero at some time, while concurrence of $2a, 2b$ rises from zero to a maximum of around 0.91. The state fidelity of $2a, 2b$ compared to the initial Bell state is around 0.958. This shows that a good entanglement transfer can be accomplished. Due to the chirality of the system, this result is independent of the distance between the qubits D . For the non-chiral case in Fig. 1(c) where $\gamma_L = \gamma_R$, the maximum concurrence is only around 0.58, even with the optimal distance of $kD = \pi$, where k is the wavenumber of the photon $k = 2\pi/\lambda$ with λ the corresponding wavelength. Comparing the fidelity of the qubit state of $2a, 2b$ (denoted $\rho_2(t)$) with the initial entangled state of $1a, 1b$ (denoted $\rho_1(0)$) such that $\mathcal{F} = \left(\text{Tr} \sqrt{\sqrt{\rho_1(0)} \rho_2(t) \sqrt{\rho_1(0)}} \right)^2$, Fig. 1(b) shows that the maximum fidelity transferred, \mathcal{F}_{max} , is around 0.951 (green dashed line), a significant improvement over the non-chiral case in Fig. 1(c) which gives $\mathcal{F}_{\text{max}} \approx 0.78$. Thus, chiral coupling drastically improves the entanglement transfer between the nodes.

To find the optimal coupling $g_1 = g_2 = g$, we plot the maximum transferred concurrence C_{max} of $2a, 2b$ against g_1 and g_2 .

As shown in Fig. 2(a), the transferred concurrence is maximal ($C_{\max} \approx 0.905$) around $g_1 = g_2 \approx 0.305\gamma_R$. Intuitively, for small couplings, the entanglement does not transfer effectively to the cavity, thus the transfer is weak. For strong couplings however, the Rabi oscillations between the cavity and the qubits become more significant, which is detrimental to the transfer of entanglement via the waveguide. It can also be seen from Fig. 2(a) that a condition for good entanglement transfer is $g_1 \sim g_2$.

To illustrate the effect of chirality on the transfer, we compare the maximum transferred concurrence for different chirality. Here, chirality is defined as $\chi \equiv (\gamma_R - \gamma_L)/(\gamma_R + \gamma_L)$. Fig. 2(b) shows the comparison for different chirality. For the fully chiral waveguide ($\chi = 1$), C_{\max} is independent of the inter-nodal distance D , as previously mentioned. This is simply due to the cascaded nature of the setup. However, when $\gamma_L \neq 0$, C_{\max} depends on the distance between the nodes. The peak at $D = 0.5\lambda$ is a result of the localisation of the photon wavefunction between the nodes [18]. The sensitivity of C_{\max} to fluctuations around this ‘sweet spot’ decreases as χ gets closer to 1. In general, the entanglement transfer worsens with decreasing chirality. Intuitively, this can be due to two factors: (i) leakage of excitation from the first node through the left port via γ_L , which decreases the probability of the second node being excited; (ii) information backflow from the second node back to the first node, which can be detrimental to the transfer process. Thus, using chirality, both problems can be addressed simultaneously, leading to good entanglement transfer.

Next, we look at the maximum transferred fidelity with different initial states of 1a, 1b. To this end, we prepare the qubits in system 1 in the state

$$|\psi_1\rangle = \cos\theta |eg\rangle + e^{i\phi} \sin\theta |ge\rangle, \quad \theta \in [0, \pi], \phi \in [0, 2\pi] \quad (4)$$

while the qubits in system 2 are initially in the ground state. The cavities are all in the vacuum state initially. From Fig. 2(c), the maximum transferred fidelity ($\mathcal{F}_{\max} = 0.951$) occurs near $\phi = 0, \theta = \pi/4$ which corresponds to the Bell state $|\Psi^+\rangle$. The case of $\mathcal{F}_{\max} = 0$ occurs near $\phi = \pi, \theta = \pi/4$ which corresponds to the Bell state $|\Psi^-\rangle$. This is because $|\Psi^-\rangle$ is a dark state of the TCM, and thus does not decay with time.

Next, we look at the initial state

$$|\psi_2\rangle = \cos\theta |gg\rangle + e^{i\phi} \sin\theta |ee\rangle, \quad \theta \in [0, 2\pi], \phi \in [-\pi, \pi] \quad (5)$$

with the Bell states $|\Phi^+\rangle = \frac{1}{\sqrt{2}}(|gg\rangle + |ee\rangle)$ and $|\Phi^-\rangle = \frac{1}{\sqrt{2}}(|gg\rangle - |ee\rangle)$. As shown in Fig. 2(d), the maximum transferred fidelity is independent of ϕ . The transferred fidelity $\mathcal{F}_{\max} \approx 0.958$ at $\theta = \pi/4, \phi = 0$ and $\theta = \pi/4, \phi = \pi$ corresponds to the Bell states $|\Psi^\pm\rangle$ respectively. The

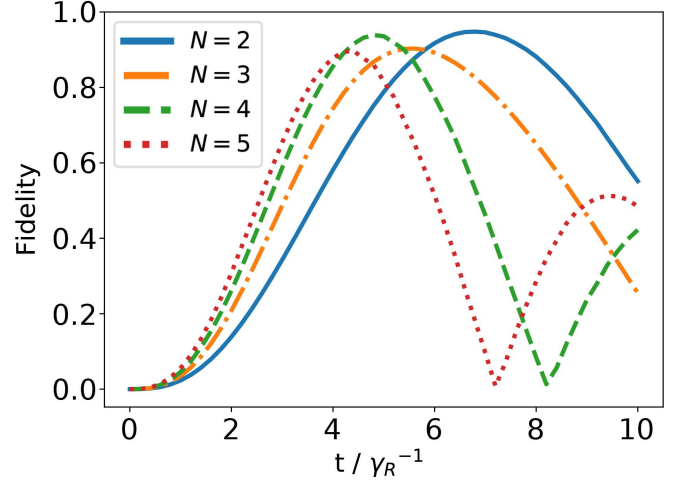


FIG. 3. Fidelity of the qubit state in cavity 2 compared to initial qubit state in cavity 1. Good transfer of W -state for different N . Other parameters are: $g_1 = g_2 = 0.3\gamma_R$, $\gamma_L = 0$, $\Gamma_j = 0$

lowest $\mathcal{F}_{\max} \approx 0.88$ occurs at $\theta = \pi/2$ which is reasonable since that corresponds to the case of transferring a two-excitation state $|ee\rangle$ to qubits initially prepared in ground state $|gg\rangle$. Overall, we have shown that good transfer of entanglement is possible for 3 out of 4 of the Bell basis states.

Transfer of multipartite entanglement with chiral couplings.—Here, we demonstrate a generalisation of the entanglement transfer scheme, by using N qubits per node. The parameters used here are the same as in Fig. 1(b) ($g_i = 0.3\gamma_R, \Gamma_{ji} = 0, \gamma_L = 0, i = 1, 2, \dots, N, j = 1, 2$). Measuring the fidelity of the qubit states in node 2 with respect to the initial state in node 1, Fig. 3 shows that the maximum fidelity transferred for a W -state of the form $|W_N\rangle = \frac{1}{\sqrt{N}}(|egg\dots g\rangle + |geg\dots g\rangle + \dots + |gg\dots ge\rangle)$ is around $\mathcal{F}_{\max} \gtrsim 0.9$, with the $N = 2$ Bell state $|\Psi^+\rangle$ reaching $\mathcal{F}_{\max} \approx 0.958$ as previously mentioned. Hence, we have demonstrated that multipartite generalisations of the W -state can be effectively transferred using the chirally-coupled waveguide.

Role of imperfections.—The analysis in the previous sections neglected qubit losses by assuming that the decay rate of the cavity is much larger than that of the qubit decay rates. Here, we look at the entanglement transfer with qubit losses. Specifically, we prepare the initial state of 1a, 2a in the Bell state $|\Psi^+\rangle$ and set all qubit decay rates to be equal ($\kappa_{jk} = \kappa$) for simplicity.

Increasing the qubit decay rate, the maximum concurrence decreases as shown in Fig. 4(b). Here, we set the inter-nodal distance to be at the ‘sweet spot’ $kD = \pi$. A comparison between the chiral ($\chi = 1$) and non-chiral ($\chi = 0$) cases shows that as long as the qubit decay rate is within $\kappa < 0.1\gamma_R$, the chiral system remains advantageous over the ideal non-chiral case in terms of entangle-

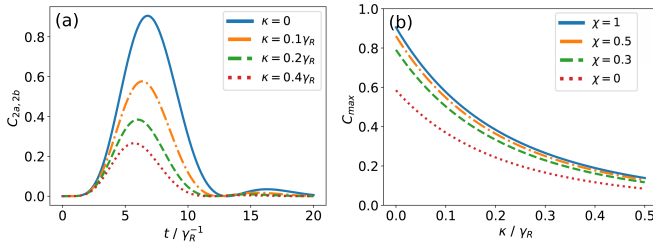


FIG. 4. Effects of qubit losses on entanglement transfer of $|\Psi^+\rangle$. (a) Concurrence of $2a, 2b$ with chiral coupling. (b) Maximum concurrence of $2a, 2b$ against qubit decay rate.

ment transfer. As mentioned earlier, the entanglement transfer at $kD = \pi$ is also relatively insensitive to small imperfections in chirality. Thus, perfect chirality is not required for the transfer scheme to work well.

Conclusion.—In this Letter, we have proposed a protocol for transferring entanglement between the two nodes in a quantum network. Our system can be easily implemented experimentally, by coupling plasmonic waveguide with ring cavities which are coupled to few atoms to realize the elementary unit of a quantum node. By considering a chiral 1D waveguide, we derived the master equation which governs the system dynamics. High-fidelity entanglement transfer is achieved by harnessing the directional asymmetry of photon emission. We have found optimal system parameters for the transfer of maximally entangled Bell states and for up to 5-qubit W -states. Our proposal requires minimal control over the system parameters contrary to other proposals which require external pulses with demanding temporal shapes [12, 23–31]. Moreover, since our entanglement transfer is achieved dynamically it is faster compared to its steady state counterparts. Finally, our protocol can easily be applied to long-distance transfer by utilising the Markovianity in cascaded systems. This can potentially be significant for the efficient distribution of entanglement within a quantum network.

The IHPC A*STAR Team would like to acknowledge the support from the National Research Foundation Singapore (Grants No. NRF2017NRFNSFC002-015, No. NRF2016-NRF-ANR002, No. NRF-CRP 14-2014-04) and A*STAR SERC (Grant No. A1685b0005). D. A., L.C. K. and J. Y. acknowledges support from National Research Foundation Singapore (Grant No. 2014NRF-CRP002-042). D. A. and W.K. M. would like to acknowledge Marc-Antoine Lemonde for helpful discussions on cascaded systems.

* waikeong_mok@u.nus.edu

[1] H. J. Kimble, *Nature* **453**, 1023 (2008).

- [2] A. Reiserer and G. Rempe, *Rev. Mod. Phys.* **87**, 1379 (2015).
- [3] M. A. Nielsen and I. Chuang, *Quantum computation and quantum information* (AAPT, 2002).
- [4] C. H. Bennett, G. Brassard, C. Crépau, R. Jozsa, A. Peres, and W. K. Wootters, *Phys. Rev. Lett.* **70**, 1895 (1993).
- [5] M. Żukowski, A. Zeilinger, M. A. Horne, and A. K. Ekert, *Phys. Rev. Lett.* **71**, 4287 (1993).
- [6] B. Coecke, arXiv preprint quant-ph/0402014 (2004).
- [7] C. H. Bennett and G. Brassard, *Theor. Comput. Sci.* **560**, 7 (2014).
- [8] A. K. Ekert, *Phys. Rev. Lett.* **67**, 661 (1991).
- [9] P. Lodahl, S. Mahmoodian, S. Stobbe, A. Rauschenbeutel, P. Schneeweiss, J. Volz, H. Pichler, and P. Zoller, *Nature* **541**, 473 (2017).
- [10] I. Söllner, S. Mahmoodian, S. L. Hansen, L. Midolo, A. Javadi, G. Kiršanskė, T. Pregolato, H. El-Ella, E. H. Lee, J. D. Song, *et al.*, *Nature nanotechnology* **10**, 775 (2015).
- [11] H. Pichler, T. Ramos, A. J. Daley, and P. Zoller, *Phys. Rev. A* **91**, 042116 (2015).
- [12] T. Ramos, B. Vermersch, P. Hauke, H. Pichler, and P. Zoller, *Phys. Rev. A* **93**, 062104 (2016).
- [13] S. Mahmoodian, P. Lodahl, and A. S. Sørensen, *Phys. Rev. Lett.* **117**, 240501 (2016).
- [14] C. Gonzalez-Ballester, A. Gonzalez-Tudela, F. J. Garcia-Vidal, and E. Moreno, *Phys. Rev. B* **92**, 155304 (2015).
- [15] H. J. Carmichael, *Phys. Rev. Lett.* **70**, 2273 (1993).
- [16] C. W. Gardiner, *Phys. Rev. Lett.* **70**, 2269 (1993).
- [17] H. Carmichael, *Statistical Methods in Quantum Optics 2: Non-Classical Fields*, Theoretical and Mathematical Physics (Springer Berlin Heidelberg, 2007).
- [18] C. Gonzalez-Ballester, F. J. García-Vidal, and E. Moreno, *New Journal of Physics* **15**, 073015 (2013).
- [19] Y.-L. L. Fang, F. Ciccarello, and H. U. Baranger, *New Journal of Physics* **20**, 043035 (2018).
- [20] J. L. O’Brien, A. Furusawa, and J. Vučković, *Nature Photonics* **3**, 687 (2009).
- [21] K. J. Vahala, *nature* **424**, 839 (2003).
- [22] T. Aoki, B. Dayan, E. Wilcut, W. P. Bowen, A. S. Parkins, T. Kippenberg, K. Vahala, and H. Kimble, *Nature* **443**, 671 (2006).
- [23] B. Vermersch, P.-O. Guimond, H. Pichler, and P. Zoller, *Phys. Rev. Lett.* **118**, 133601 (2017).
- [24] J. I. Cirac, P. Zoller, H. J. Kimble, and H. Mabuchi, *Phys. Rev. Lett.* **78**, 3221 (1997).
- [25] G. M. Nikolopoulos, I. Jex, *et al.*, *Quantum state transfer and network engineering* (Springer, 2014).
- [26] C. Dłaska, B. Vermersch, and P. Zoller, *Quantum Science and Technology* **2**, 015001 (2017).
- [27] K. Stannigel, P. Rabl, A. S. Sørensen, P. Zoller, and M. D. Lukin, *Phys. Rev. Lett.* **105**, 220501 (2010).
- [28] K. Stannigel, P. Rabl, A. S. Sørensen, M. D. Lukin, and P. Zoller, *Phys. Rev. A* **84**, 042341 (2011).
- [29] N. Y. Yao, C. R. Laumann, A. V. Gorshkov, H. Weimer, L. Jiang, J. I. Cirac, P. Zoller, and M. D. Lukin, *Nature communications* **4**, 1585 (2013).
- [30] H. Zheng and H. U. Baranger, *Phys. Rev. Lett.* **110**, 113601 (2013).
- [31] T. van Leent, M. Bock, R. Garthoff, K. Redeker, W. Zhang, T. Bauer, W. Rosenfeld, C. Becher, and

- H. Weinfurter, arXiv preprint arXiv:1909.01006 (2019).
- [32] J. Hofmann, M. Krug, N. Ortegel, L. Gérard, M. Weber, W. Rosenfeld, and H. Weinfurter, *Science* **337**, 72 (2012).
- [33] S. Ritter, C. Nölleke, C. Hahn, A. Reiserer, A. Neuzner, M. Uphoff, M. Mücke, E. Figueroa, J. Bochmann, and G. Rempe, *Nature* **484**, 195 (2012).
- [34] W. Rosenfeld, D. Burchardt, R. Garthoff, K. Redeker, N. Ortegel, M. Rau, and H. Weinfurter, *Phys. Rev. Lett.* **119**, 010402 (2017).
- [35] S. Bose, *Contemporary Physics* **48**, 13 (2007).
- [36] M. Rafiee, M. Soltani, H. Mohammadi, and H. Mokhtari, *The European Physical Journal D* **63**, 473 (2011).
- [37] A. Bayat and S. Bose, *Advances in Mathematical Physics* **2010** (2010).
- [38] R. Sousa and Y. Omar, *New Journal of Physics* **16**, 123003 (2014).
- [39] Y.-H. Ji and Y.-M. Liu, *Optik* **126**, 2414 (2015).
- [40] Z.-X. Man, N. B. An, Y.-J. Xia, and J. Kim, *Physics Letters A* **378**, 2063 (2014).
- [41] R. Vieira and G. Rigolin, *Physics Letters A* **382**, 2586 (2018).
- [42] D. E. Chang, A. S. Sørensen, P. R. Hemmer, and M. D. Lukin, *Phys. Rev. Lett.* **97**, 053002 (2006).
- [43] A. V. Akimov, A. Mukherjee, C. L. Yu, D. E. Chang, A. S. Zibrov, P. R. Hemmer, H. Park, and M. D. Lukin, *Nature* **450**, 402 EP (2007).
- [44] D. Martín-Cano, A. González-Tudela, L. Martín-Moreno, F. J. García-Vidal, C. Tejedor, and E. Moreno, *Phys. Rev. B* **84**, 235306 (2011).

Appendix A: Derivation of the effective master equation

In this Appendix, we derive the effective master equation from tracing out the degree of freedoms of the common bath, which in this case is the 1D waveguide. Note that this derivation is similar to the approach taken in [23]. For simplicity, we assume here that the qubits do not decay, and that the ring resonators are at a common frequency ω_c . From the Hamiltonian in Eq. (1), and choosing a frame rotating with the cavity and bath, i.e. $U = \exp[i(\sum_j \omega_{cj} a_j^\dagger a_j + \sum_\lambda \int d\omega \omega b_\lambda^\dagger(\omega) b_\lambda(\omega))]$ and applying the transformation $H = UH U^\dagger - i\dot{U}U^\dagger$, we have

$$\tilde{H}_{SB}(t) = i \sum_{\lambda,j} \int d\omega \sqrt{\frac{\gamma_\lambda}{2\pi}} \left(b_\lambda^\dagger(\omega) a_j e^{i(\omega-\omega_c)t} e^{-i\omega x_j/v} - e^{i(\omega-\omega_c)t} e^{i\omega x_j/v} a_j^\dagger b_\lambda(\omega) \right) \quad (6)$$

From Heisenberg equations of motion, we have

$$\dot{b}_\lambda(\omega, t) = i[H, b_\lambda(\omega, t)] = \sum_{j=1,2} \sqrt{\frac{\gamma_\lambda}{2\pi}} a_j(t) e^{i(\omega-\omega_c)t} e^{-i\omega x_j/v} \quad (7)$$

which can be formally integrated to obtain

$$b_\lambda(\omega, t) = b_\lambda(\omega, 0) + \int_0^t ds \sum_j \sqrt{\frac{\gamma_\lambda}{2\pi}} a_j(s) e^{i(\omega-\omega_c)s} e^{-i\omega x_j/v} \quad (8)$$

For an arbitrary system operator $X(t)$, the Heisenberg equation reads

$$\dot{X}(t) = \sum_{\lambda,j} \int d\omega \sqrt{\frac{\gamma_\lambda}{2\pi}} (b_\lambda^\dagger(\omega, t) e^{i(\omega-\omega_c)t} e^{-i\omega x_j/v} [X(t), a_j(t)] - b_\lambda(\omega, t) e^{-i(\omega-\omega_c)t} e^{i\omega x_j/v} [X(t), a_j^\dagger(t)]) \quad (9)$$

Substituting $b_\lambda(\omega, t)$ into $\dot{X}(t)$ and defining $b_\lambda(t) \equiv \frac{1}{\sqrt{2\pi}} \int d\omega b_\lambda(\omega) e^{-i(\omega-\omega_c)t}$ and $k = \omega_0/v$, we have

$$\begin{aligned} \dot{X}(t) = & \sum_{\lambda,j} \sum_{\lambda,j} \sqrt{\gamma_\lambda} b_\lambda^\dagger(t - x_j/v) e^{-ikx_j} [X(t), a_j(t)] - [X(t), a_j^\dagger(t)] b_\lambda(t - x_j/v) e^{ikx_j} \\ & + \sum_{\lambda,j,l} \frac{\gamma_\lambda}{2\pi} \int_0^t ds \int d\omega e^{i(\omega-\omega_c)(t-s)} e^{-i\omega x_{jl}/v} a_l^\dagger(s) [X(t), a_j(t)] - e^{-i(\omega-\omega_c)(t-s)} e^{i\omega x_{jl}/v} a_l(s) [X(t), a_j^\dagger(t)] \end{aligned} \quad (10)$$

We can perform the Born-Markov approximation by treating the time delay x_{jl}/v between the two atoms to be very small. Thus,

$$\begin{aligned} \sum_l \frac{1}{2\pi} \int_0^t ds \int d\omega e^{i(\omega-\omega_j)(t-s)} e^{-i\omega x_{jl}/v} a_l^\dagger(s) &= \sum_l \int_0^t ds \delta(t - x_{jl}/v - s) e^{-ikx_{jl}} a_l^\dagger(s) \\ &\approx \frac{1}{2} a_l^\dagger(t) + \sum_l \theta(x_{jl}/v) e^{-ikx_{jl}} a_l^\dagger(t) \end{aligned} \quad (11)$$

where the first term is the contribution from $x_{jl}/v < 0$ and the second term is from $x_{jl}/v > 0$. The Markov approximation is also applied to the second term $\sigma_l^\dagger(t - x_{jl}/v) \rightarrow \sigma_l^\dagger(t)$.

Next, we substitute this into the equation for $\dot{X}(t)$ and take average. Since the bath is initially in the vacuum, $\langle b_\lambda(t) \rangle = 0$. Thus,

$$\begin{aligned} \langle \dot{X}(t) \rangle &= \sum_{\lambda j} \frac{\gamma_\lambda}{2} \left(\langle a_j^\dagger(t) [X(t), a_j(t)] \rangle - \langle [X(t), a_j^\dagger(t)] a_j(t) \rangle \right) \\ &\quad + \sum_{\lambda j l, x_j > x_l} \gamma_\lambda \left(e^{-ikx_{jl}} \langle a_l^\dagger(t) [X(t), a_j(t)] \rangle - e^{ikx_{jl}} \langle [X(t), a_j^\dagger(t)] a_l(t) \rangle \right) \end{aligned} \quad (12)$$

To obtain the master equation, we first note that the average is the same in both Schrodinger picture and Heisenberg picture, thus $\text{Tr}(X(t)\rho(0)) = \text{Tr}(X\rho(t))$, that is, we can transfer the time dependence from system operator to density operator. For example, the first term on the RHS can be written as

$$\langle a_j^\dagger(t) [X(t), a_j(t)] \rangle = \text{Tr}(a_j^\dagger X a_j \rho(t) - a_j X a_j^\dagger \rho(t)) = \text{Tr}(X [a_j, \rho(t) a_j^\dagger]) \quad (13)$$

using the cyclic property of trace. Doing this for all the terms and noting that the equation holds for all $X(t)$, we have

$$\dot{\rho}(t) = -i[H_S, \rho(t)] + \sum_{\lambda j} \frac{\gamma_\lambda}{2} ([a_j, \rho(t) a_j^\dagger] - [a_j^\dagger, a_j \rho(t)]) + \sum_{\lambda j l, x_j > x_l} \gamma_\lambda \left(e^{-ikx_{jl}} [\sigma_j, \rho(t) a_l^\dagger] - e^{ikx_{jl}} [a_j^\dagger, a_l \rho(t)] \right) \quad (14)$$

where the last term describe the effective long-range interactions between the two resonators mediated by the waveguide.